



# Numerical Investigation of Flow and Starting Characteristics of Nozzle-Diffuser System for Plasma Wind Tunnel

---

**Daesan Choi\* and Kyu-Hong Kim\*\***

**\* R&D Center, NEXTfoam CO., LTD., Seoul, South Korea**

**\*\* Department of Mechanical and Aerospace Engineering,  
Seoul National University, Seoul, South Korea**





# Outline

- 1. Background**
- 2. Materials and Methods**
- 3. Flow Analysis of Nozzle-Diffuser System**
- 4. Starting Characteristics**
- 5. Conclusion**

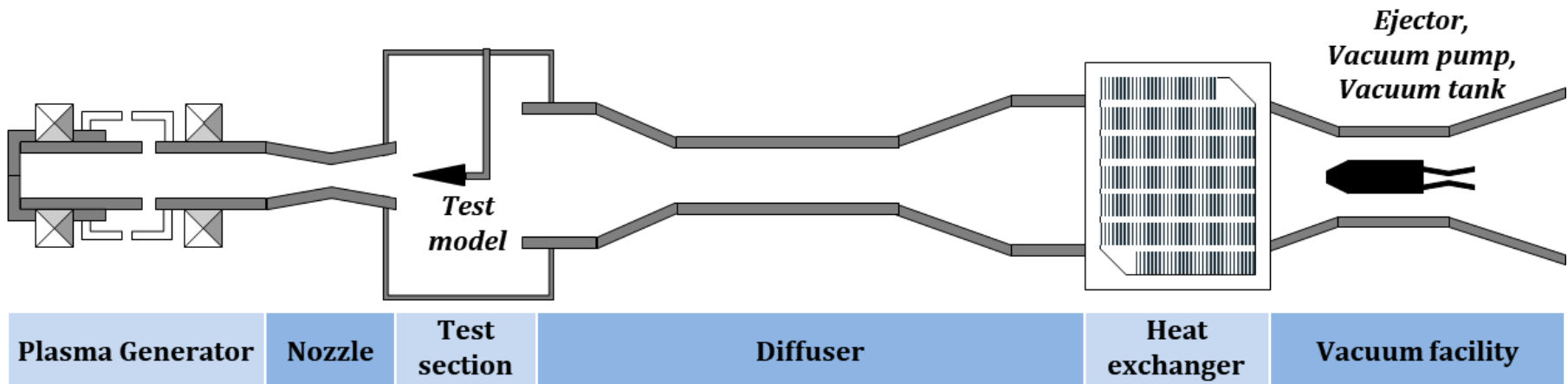


# Background



# Plasma Wind Tunnel (PWT)

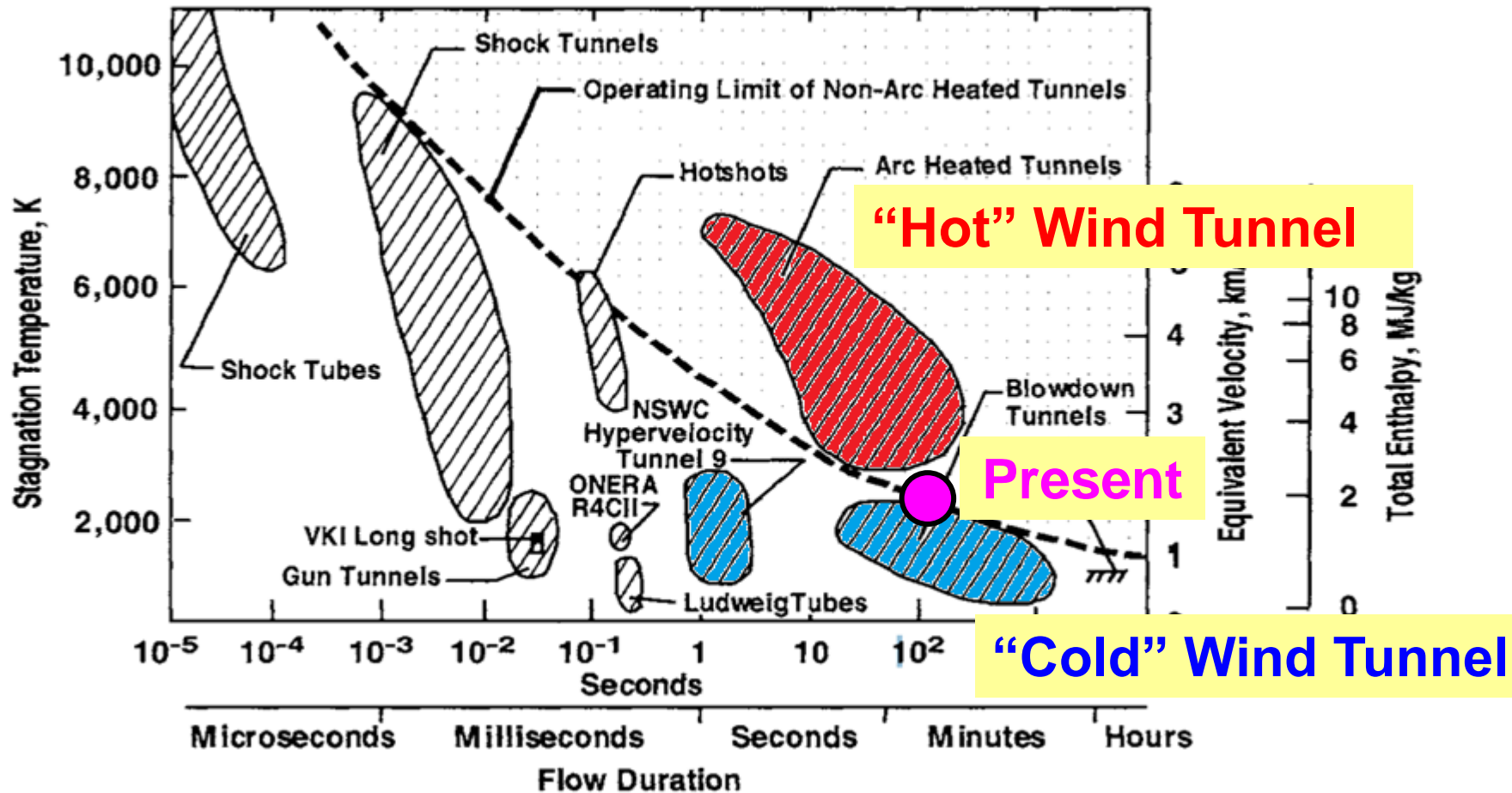
- Simulating **hypersonic/high enthalpy** flows
- Additional components with high power
  - **Plasma generator**
  - **Cooling system, ejector, vacuum facility**



< Schematic of a plasma wind tunnel >



# Type of Wind Tunnel



< Capabilities of aerothermal facility [1] >



# Characteristics of PWT

- **Low Reynolds number**
  - $Re_D = 10^4 \sim 10^6$  (*vs.*  $10^5 \sim 10^7$  in SWT)
  - **Viscous dominant / Damped shock wave**

**Re = 3,000**

**Damped shock wave**



**Re = 30,000**

**Sharply defined shock wave**



< Pressure contour difference according to Reynolds number [2] >



# Characteristics of PWT

- **Far higher pressure ratio required [2, 3]**
  - Owing to shock wave, dominant viscous effect
- **May requiring long time test duration [4, 5]**
  - Ablation, Reentry test

< Difference between general SWT and PWT >

	Pressure Ratio	Test Duration	Reynolds Number ( $Re_D = \frac{\rho_\infty V_\infty D}{\mu_\infty}$ )
<b>SWT</b>	$10^0 \sim 10^2$	$10^1 \sim 10^2$ sec.	$10^5 \sim 10^7$
<b>PWT</b>	$10^2 \sim 10^3$	$10^0 \sim 10^3$ sec.	$10^2 \sim 10^5$ (Present $2 \times 10^4$ )



# Motivation

- **Prediction of pressure ratio**
  - Most of literature dealing with it
  - **Key design parameter** to determine
    - (1) the type and spec. of the **plasma generator**
    - (2) **vacuum facility** capacity and spec.
    - (3) whether to use a boosting **ejector**
  - Difficulties caused by flow characteristics [2, 6]
- **Limited literature and information of PWT**
  - Frequently mentioned this limitation [2, 5, 6, 7]



# Motivation

- **Wind tunnel start**
  - Shock wave pushed downstream
  - **Sufficient pressure ratio** pushing shock wave

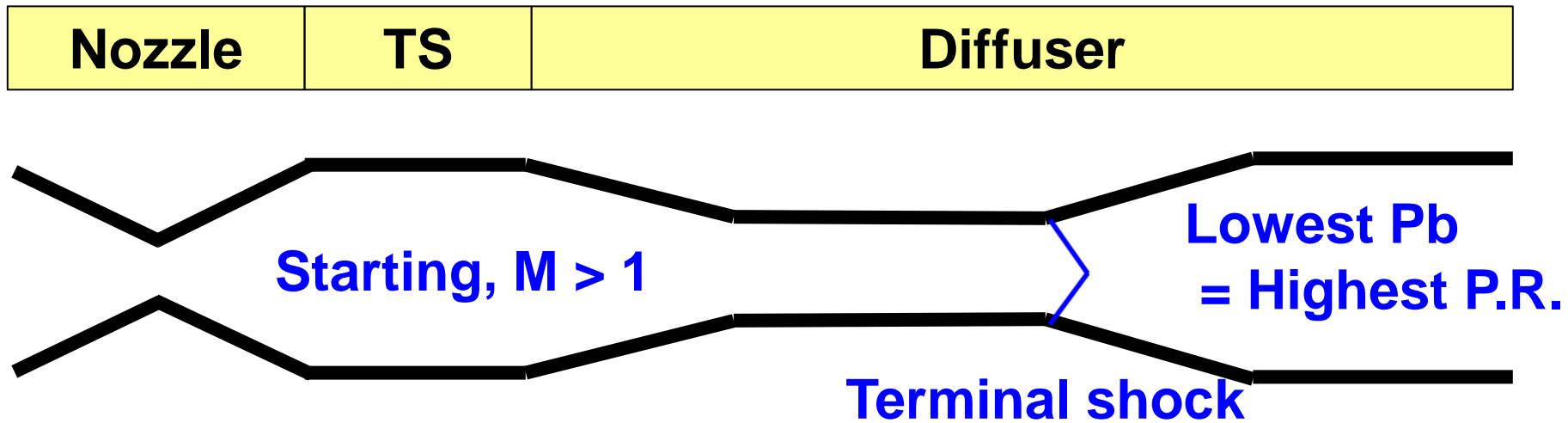


< Under-expanded (left) and over-expanded (right) jet of GHIBLI PWT [8] >



# Motivation

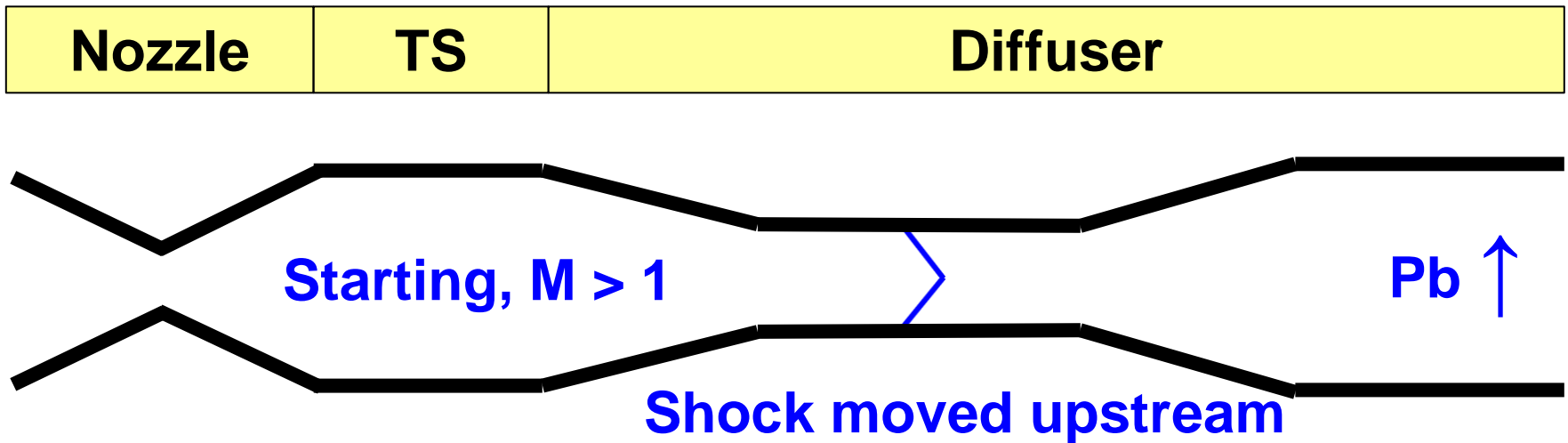
- Literature mainly focused on **minimum operable pressure ratio**
  - Initially **assume wind tunnel already started**
  - Initial condition with very low back-pressure





# Motivation

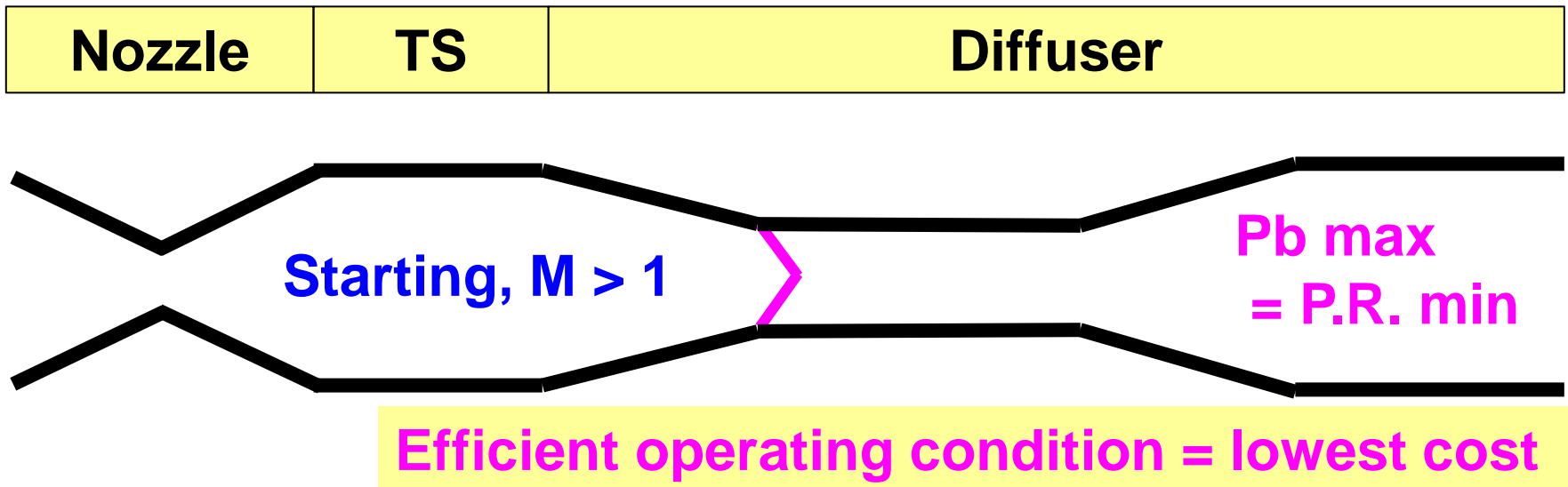
- Literature mainly focused on **minimum operable pressure ratio**
  - Gradually increasing back-pressure





# Motivation

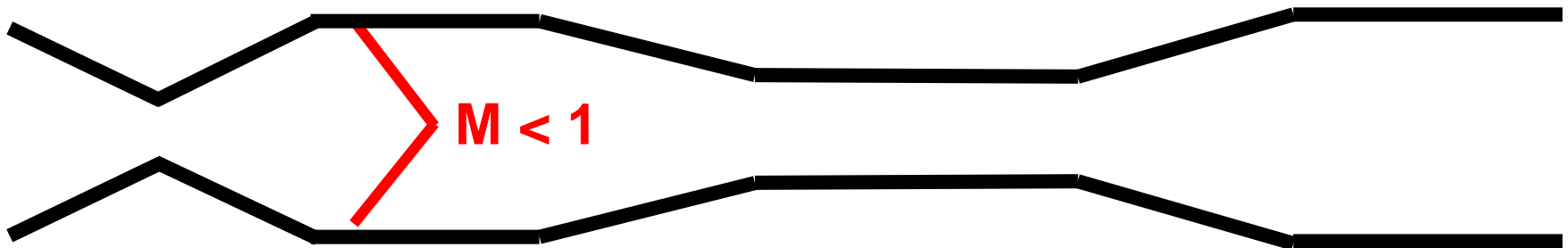
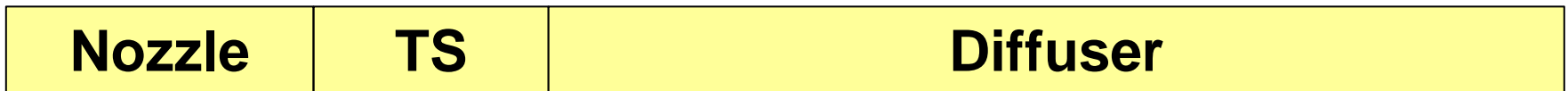
- Literature mainly focused on **minimum operable pressure ratio**
  - Gradually increasing back-pressure
  - **Until the un-starting**





# Motivation

- Literature mainly focused on **minimum operable pressure ratio**
  - **Pressure ratio for operation** is important
  - Necessary to consider **starting pressure ratio**



Inoperable

How much P.R. to push the shock?



# Objectives

- **Numerical Investigation of the flow in PWT**
  - Shock train, terminal shock
  - **Flow variables including total pressure**
- **Investigate starting characteristics**
  - Decreasing / Increasing back-pressure
  - Identifying
    - (1) maximum operable back-pressure
    - (2) **starting back-pressure**
    - (3) **hysteresis**



# Materials and Methods



# Governing Equations

- **Axisymmetric Reynolds Averaged Navier-Stokes (RANS) Equations**

$$\frac{\partial Q}{\partial t} + \frac{\partial E}{\partial x} + \frac{\partial F}{\partial y} + H = \frac{\partial E_v}{\partial x} + \frac{\partial F_v}{\partial y} + H_v$$

**Conservative Variables**

$$Q = \begin{bmatrix} \rho \\ \rho u \\ \rho v \\ \rho e_t \end{bmatrix}$$

**Convective and Diffusive Flux**

$$E = \begin{bmatrix} \rho u \\ \rho u^2 + p \\ \rho uv \\ (\rho e_t + p)u \end{bmatrix}, F = \begin{bmatrix} \rho v \\ \rho uv \\ \rho v^2 + p \\ (\rho e_t + p)v \end{bmatrix}$$

**Additional Axisymmetric terms**

$$H = \frac{1}{y} \begin{bmatrix} \rho u \\ \rho uv \\ \rho v^2 \\ (\rho e_t + p)v \end{bmatrix}$$

$$E_v = \begin{bmatrix} 0 \\ \tau_{xx} \\ \tau_{xy} \\ u\tau_{xx} + v\tau_{xy} - q_x \end{bmatrix}, F_v = \begin{bmatrix} 0 \\ \tau_{xy} \\ \tau_{yy} \\ u\tau_{xy} + v\tau_{yy} - q_y \end{bmatrix}$$

$$H_v = \begin{bmatrix} 0 \\ (h_v)_2 \\ (h_v)_3 \\ (h_v)_4 \end{bmatrix}$$



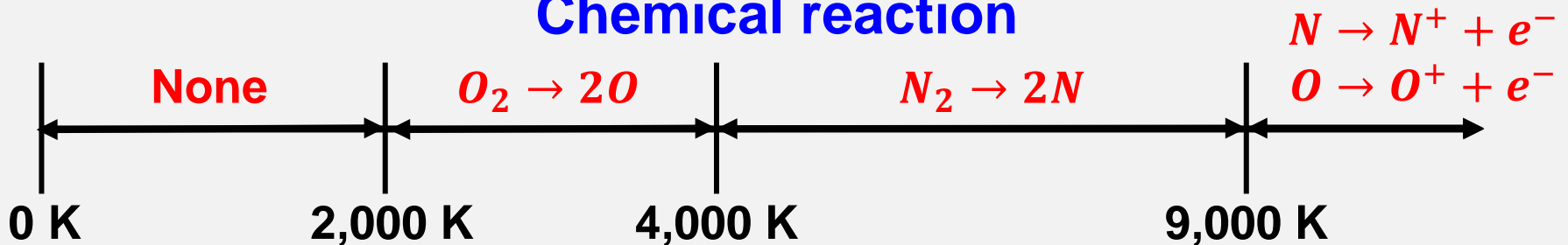
# Modeling of Equilibrium

- (Air) Internal temperature up to **2,500K**
  - Vibrational excitation, chemical reaction occur [9]

## Mode of energy

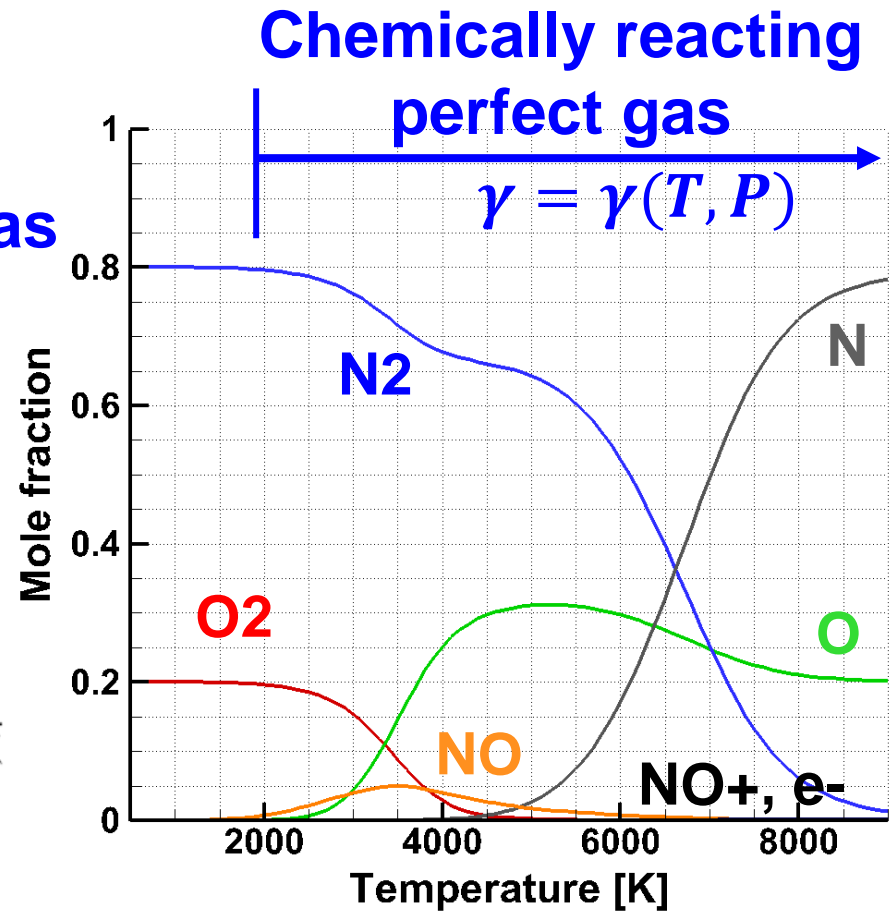
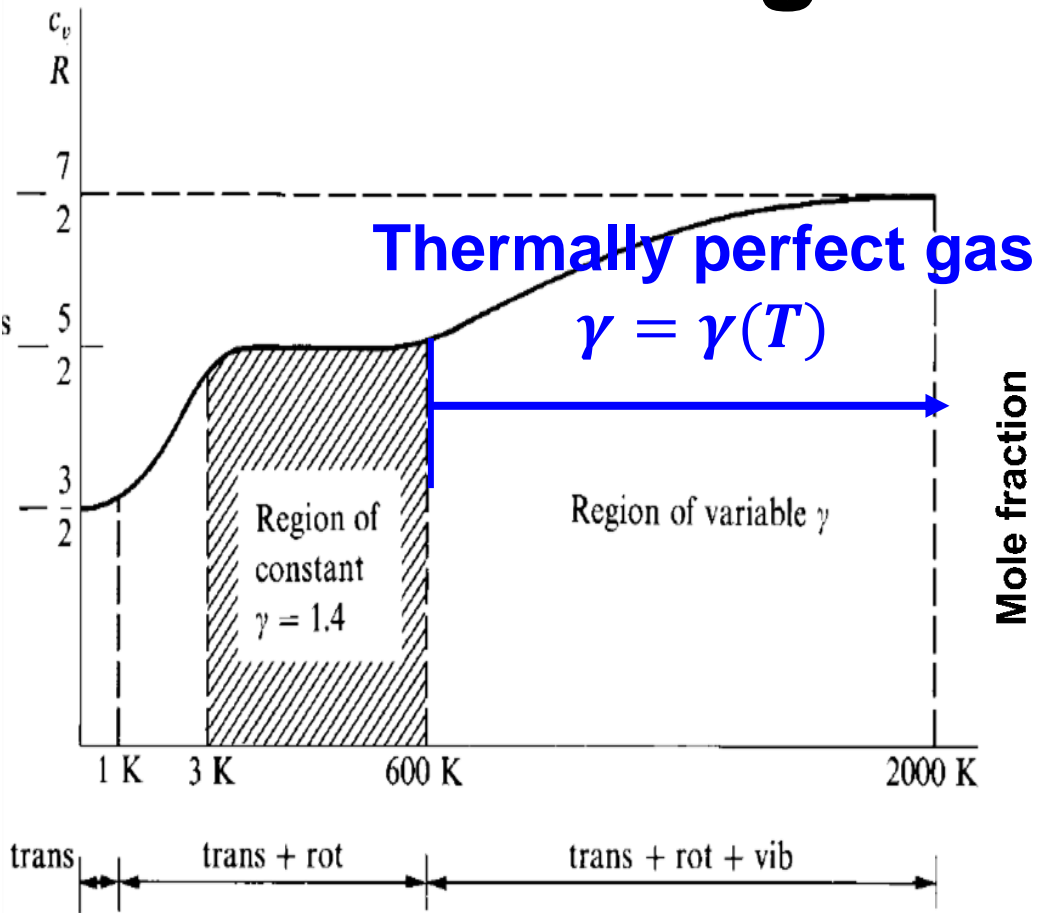


## Chemical reaction





# Modeling of Equilibrium

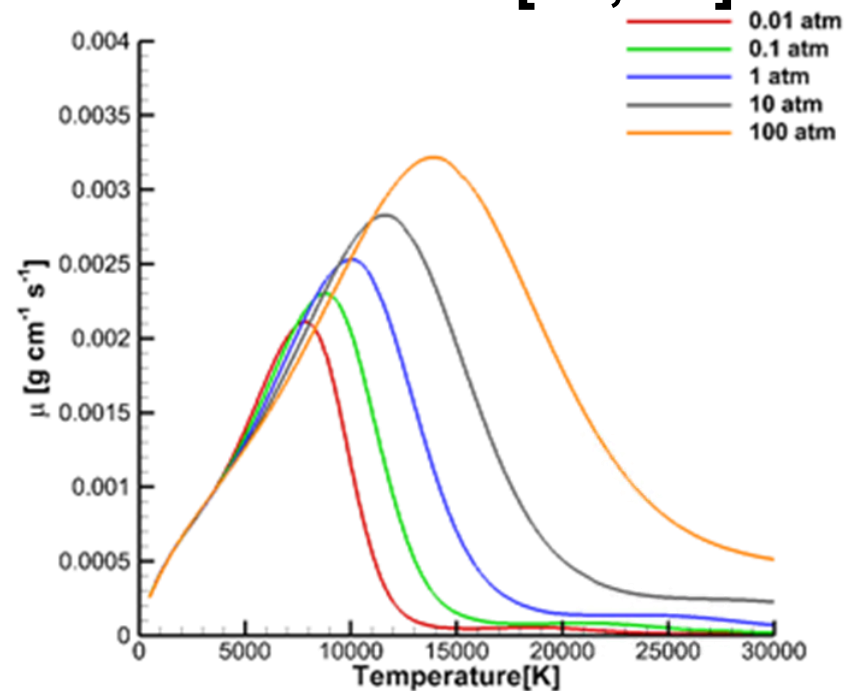
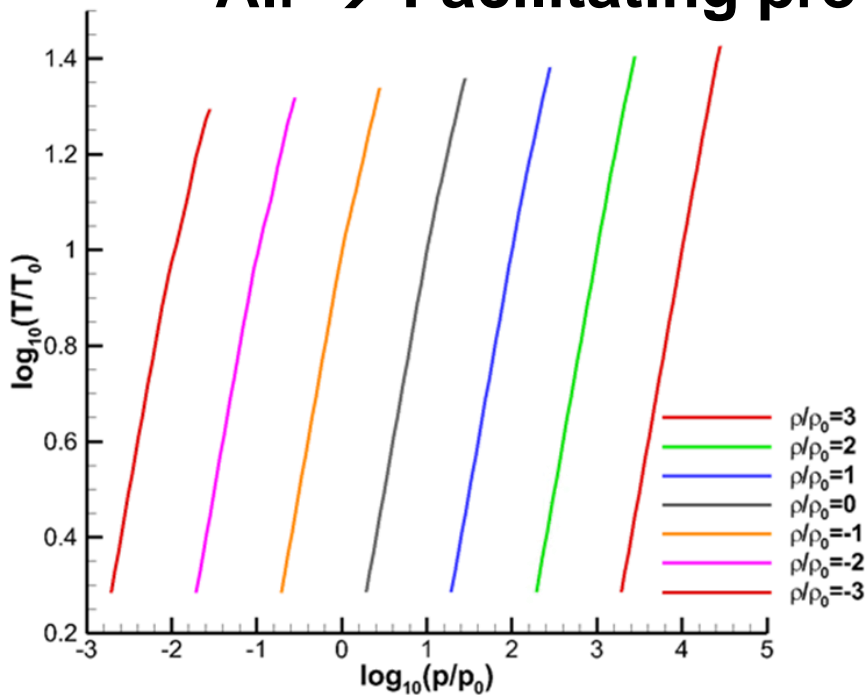


< Variation of specific heat (left) [9] and composition of air (right) >



# Modeling of Equilibrium

- Assume **thermal and chemical equilibrium**
  - Air → Facilitating pre-established data [10, 11]



< Examples of equilibrium properties of air calculated from correlation >



# Modeling of Turbulence

- **Standard k-epsilon turbulence model [12]**
  - **Used in related literatures [4, 6]**
  - **Applicable to wall bounded internal flow**

$$\frac{\partial(\rho k)}{\partial t} + \nabla \cdot (\rho k \vec{V}) = \nabla \cdot \left[ \left( \mu_l + \frac{\mu_t}{\sigma_k} \right) \nabla k \right] - \rho \varepsilon + 2\mu_t \overline{\overline{\vec{E} \cdot \vec{E}}}$$

$$\frac{\partial(\rho \varepsilon)}{\partial t} + \nabla \cdot (\rho \varepsilon \vec{V}) = \nabla \cdot \left[ \left( \mu_l + \frac{\mu_t}{\sigma_\varepsilon} \right) \nabla \varepsilon \right] + C_1 \frac{\varepsilon}{k} 2\mu_t \overline{\overline{\vec{E} \cdot \vec{E}}} - C_2 \rho \frac{\varepsilon^2}{k}$$

$$\sigma_k = 1.00, \sigma_\varepsilon = 1.3, C_1 = 1.44, C_2 = 1.92, C_\mu = 0.09$$

$$\mu_T = C_\mu \frac{\rho k^2}{\varepsilon}$$

$$\mu = \mu_L + \mu_T$$



# Computation

- **Mass flow rate difference less than 1 %**
- **Step-by-step steady calculations [2]**

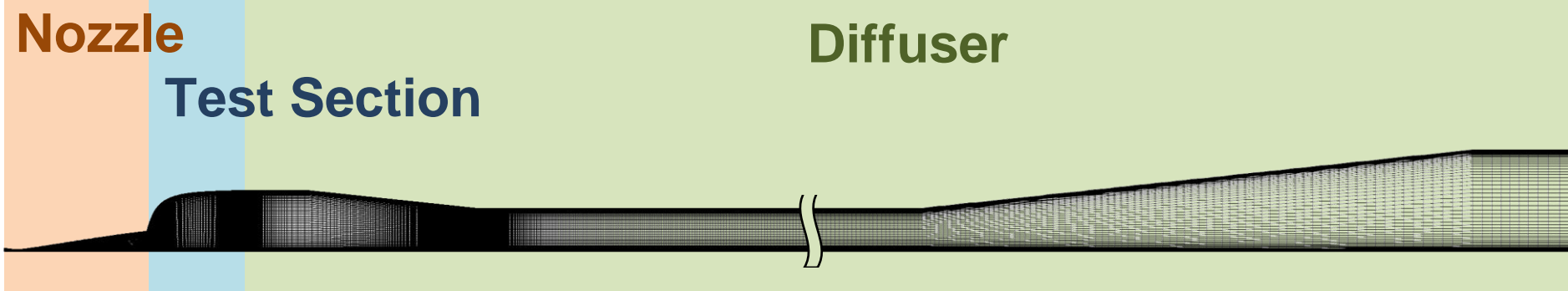
< Numerical schemes used in the study >

<b>Numerical scheme</b>	
<b>Convective flux Differencing</b>	<b>AUSMPW+ [13]</b>
<b>Spatial Reconstruction</b>	<b>TVD with minmod limiter [14]</b>
<b>Pseudo time Integration</b>	<b>LU-SGS [15]</b>



# Computational Domain

- **Mach 7 Nozzle – Test section – Diffuser**
- **Structured mesh (quadrilateral)**
  - Node dimension: 1510 X 91
  - Y+ less than 1.0 near the wall ( $y^+ \sim 0.5$ )

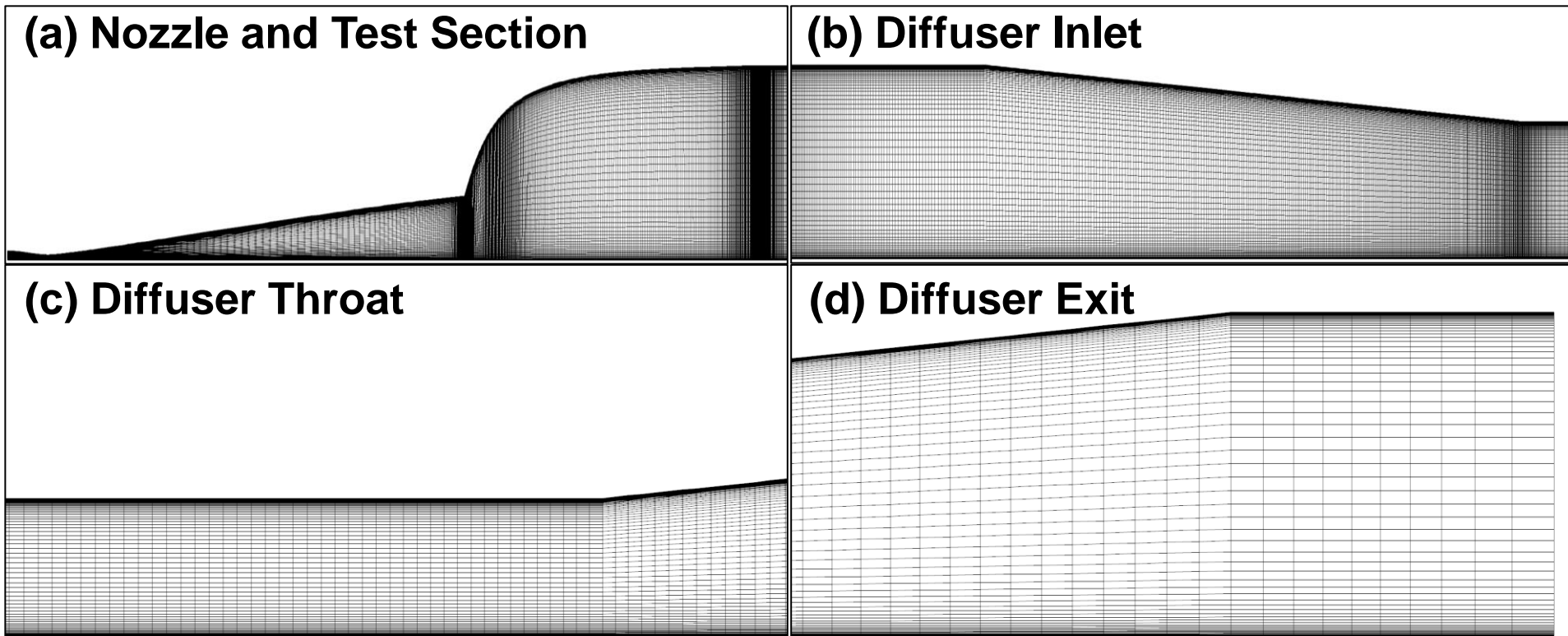


< Computational domain >



# Computational Domain

- **Grid configurations of each parts**



< Grid configuration of each parts >

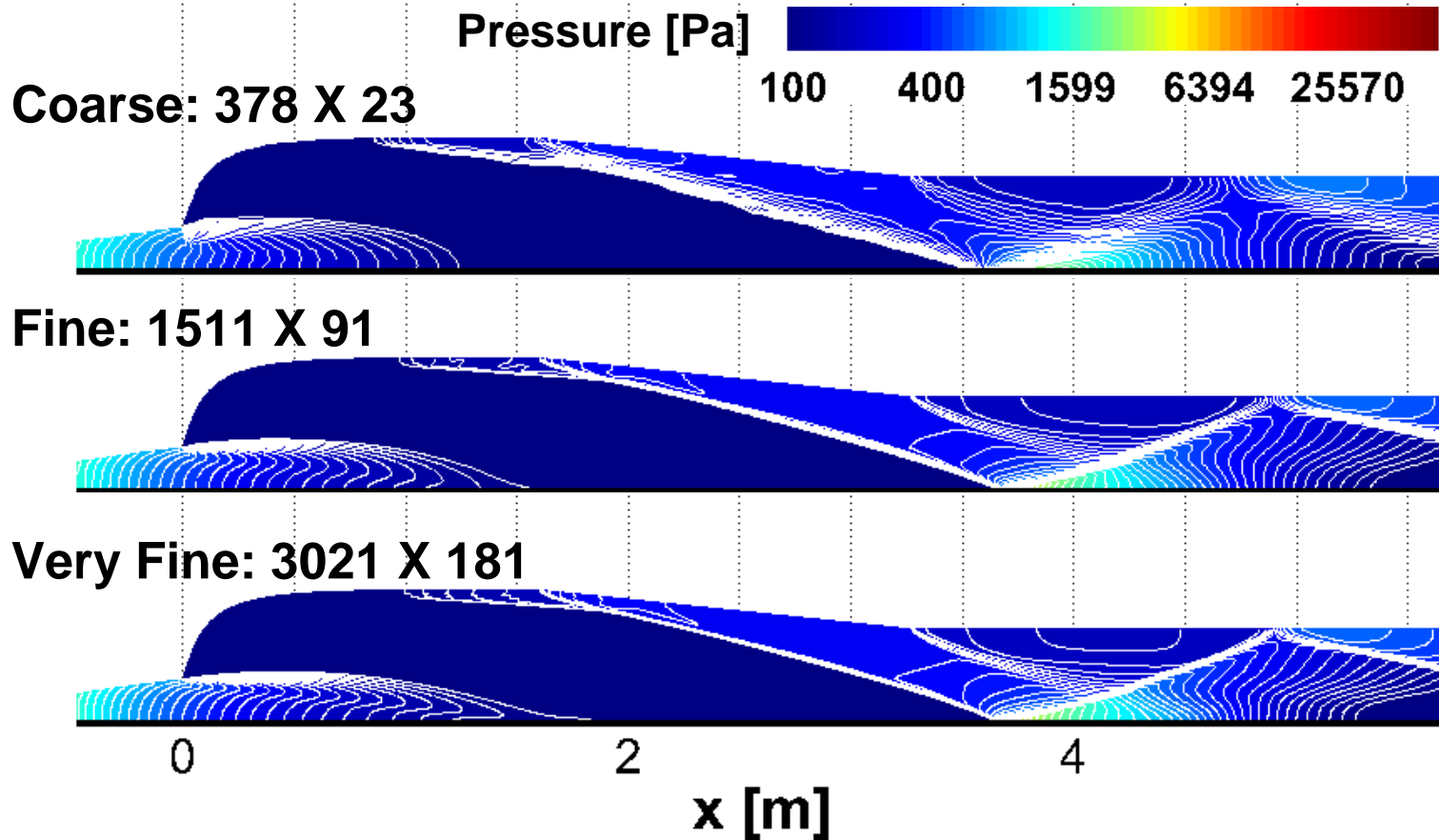


# Grid Convergence Study

- **Grid dimension considered**
  - **Double refined with distribution rules maintained**
  - **378 X 23 / 756 X 46 / 1511 X 91 / 3021 X 181**
- **Convergence check on**
  - **Shock wave configuration**
  - **Axial distributions of flow variables**  
(Mach number, static pressure, total pressure)



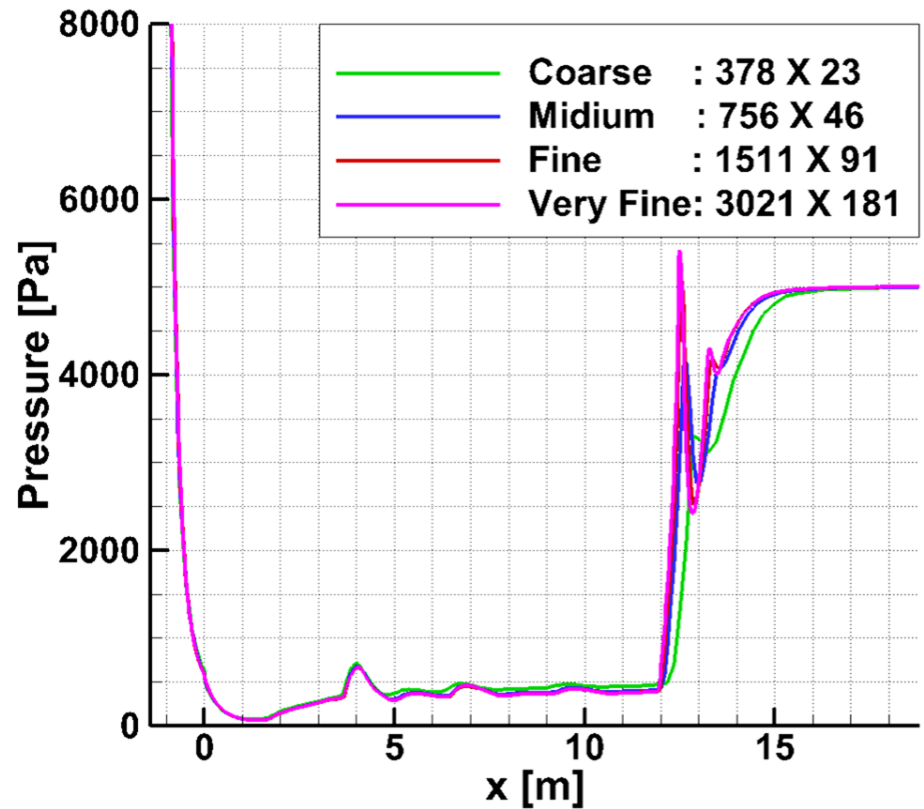
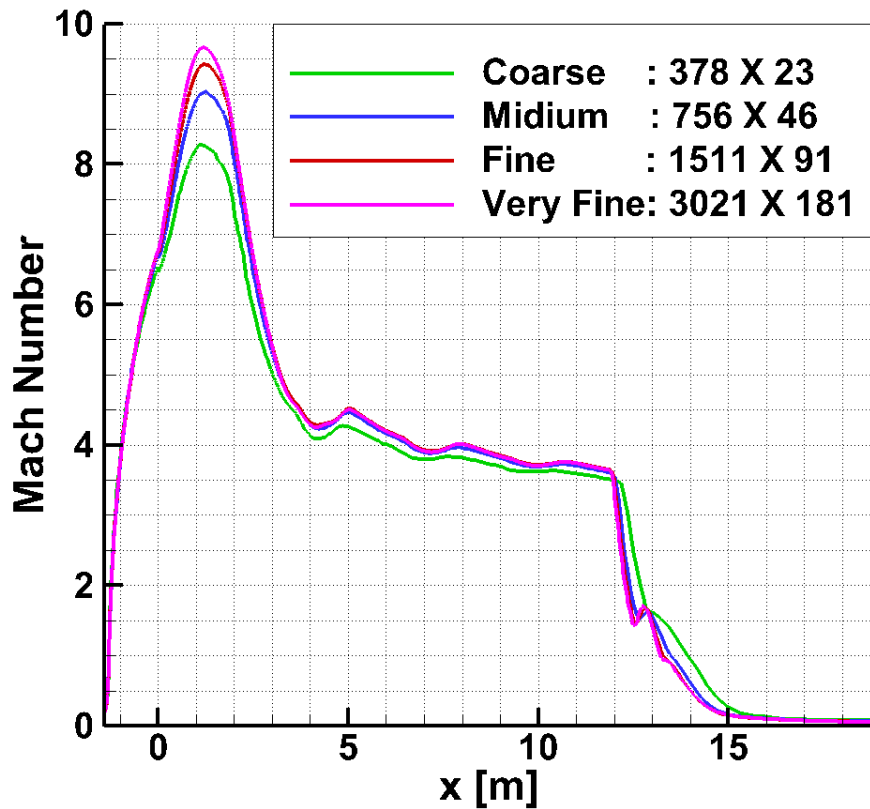
# Grid Convergence Study



< Shock wave configurations with various grid levels >



# Grid Convergence Study

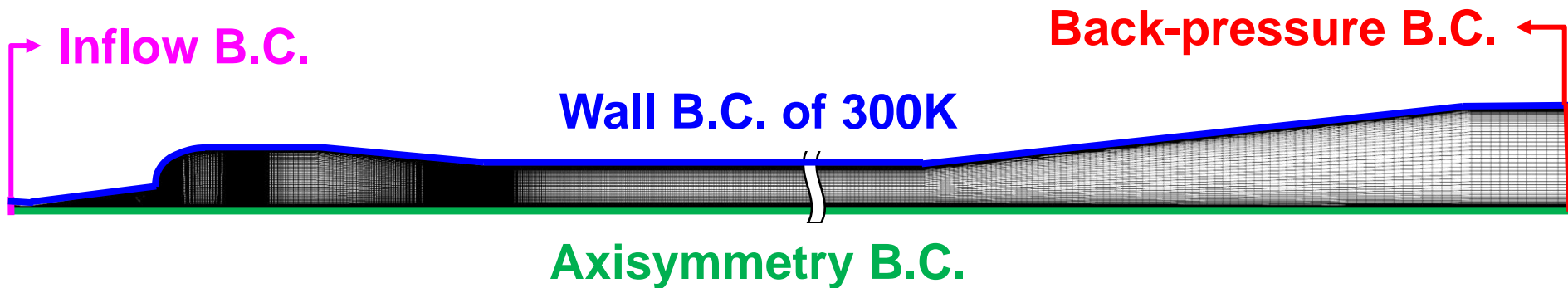


< Mach number (left) and pressure (right) distributions with various grid levels >



# Inflow / Boundary Conditions

- (Wall) Constant temperature of 300K
- (Diffuser exit) Constant back-pressure
  - Varying back-pressure → control pressure ratio
- Axisymmetry



< Boundary conditions applied >



# Inflow / Boundary Conditions

- (Inflow) NASA Langley AHSTF [16]
  - 13MW Arc-Heated Scramjet Test Facility
  - Based on reservoir condition of Mach 6
  - Replace Mach 6 nozzle with Mach 7 nozzle

< Inflow conditions and Nozzle exit Mach number >

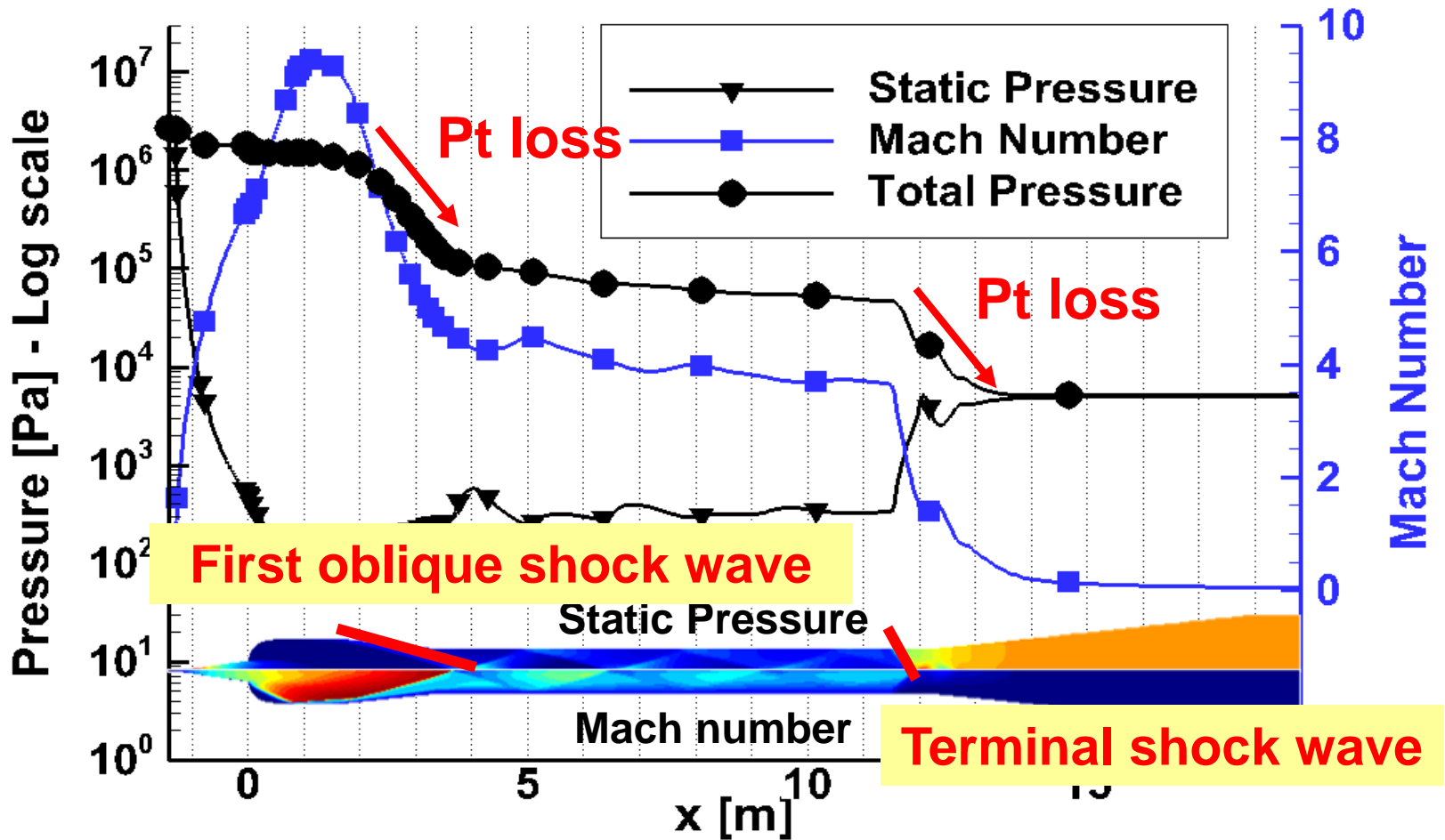
Nozzle inlet (Inflow B.C.)	$P_0$	28.6 bar
	$T_0$	2216 K
	$\dot{m}$	2.04 kg/s
Nozzle exit	M	7.0



# Flow Analysis of Nozzle-Diffuser System



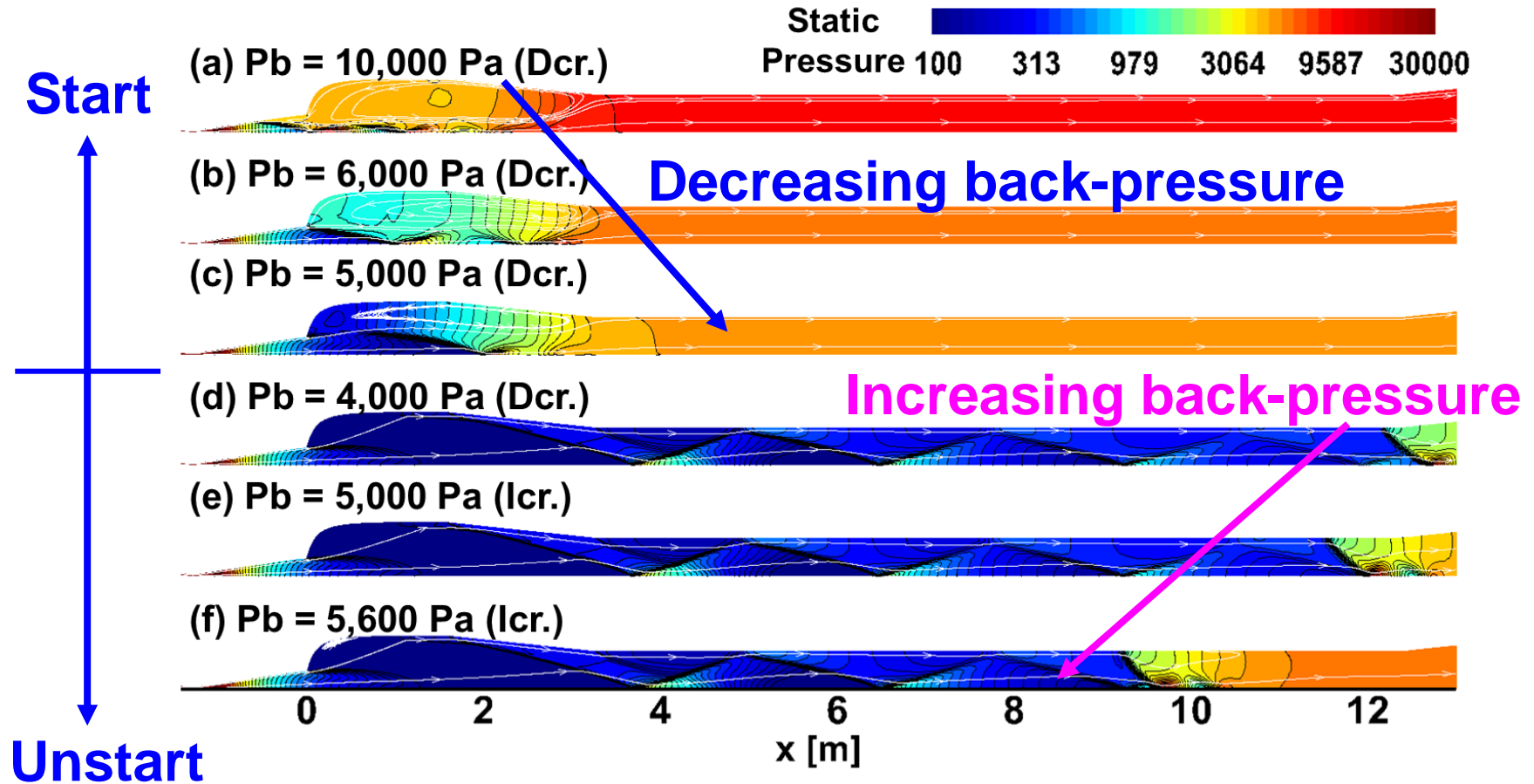
# Flow Distribution (General Aspect)



< Flow distributions of pressure, Mach number, and total pressure >



# Varying Back-pressures

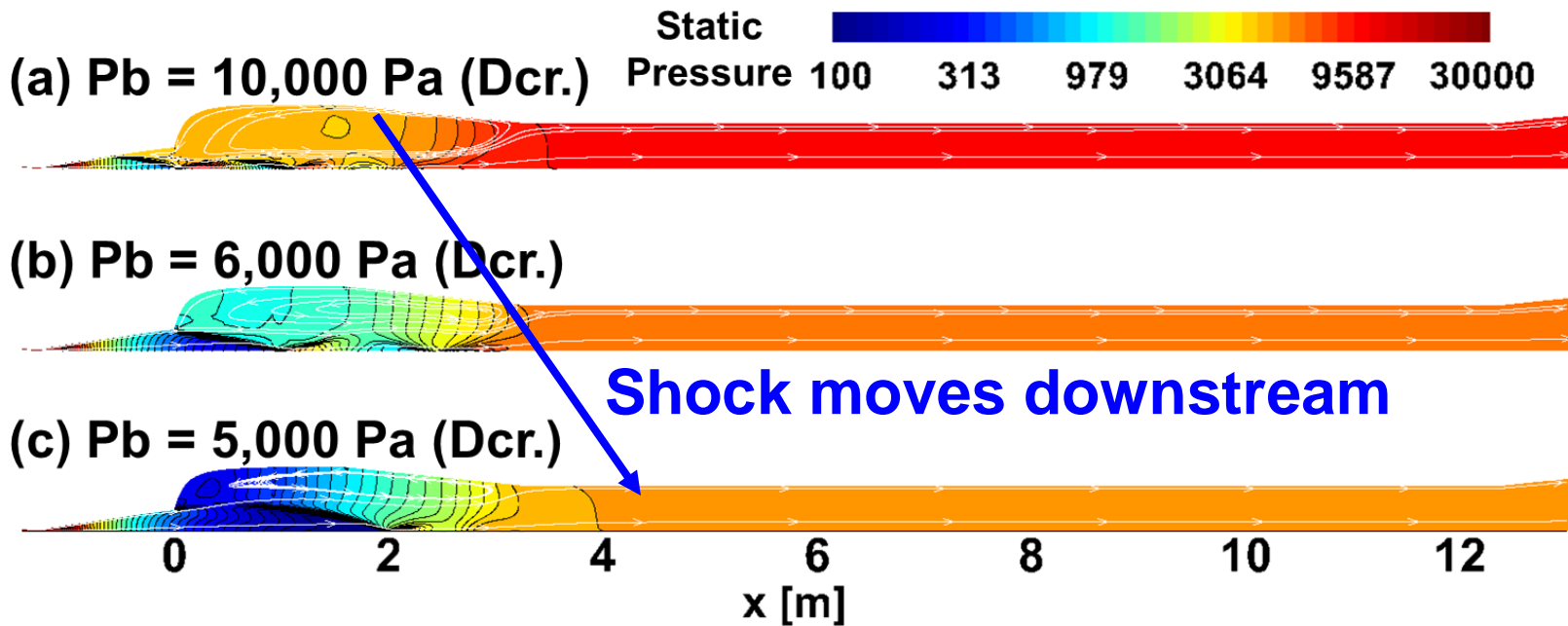


< Pressure distribution with different back-pressure >



# Varying Back-pressures

- **Decreasing back-pressure**
  - Before wind tunnel starting

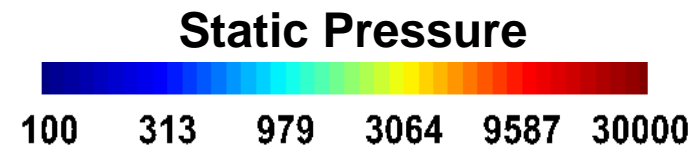


< Pressure distribution with different back-pressure (Decreasing) >



# Varying Back-pressures

- **Decreasing back-pressure**
  - **Decreasing TS pressure**



(a)  $P_b = 10,000 \text{ Pa}$  (Dcr.)

**Shock in nozzle**



(b)  $P_b = 6,000 \text{ Pa}$  (Dcr.)

**Over-expanded jet**



-1                      0                      1                      2

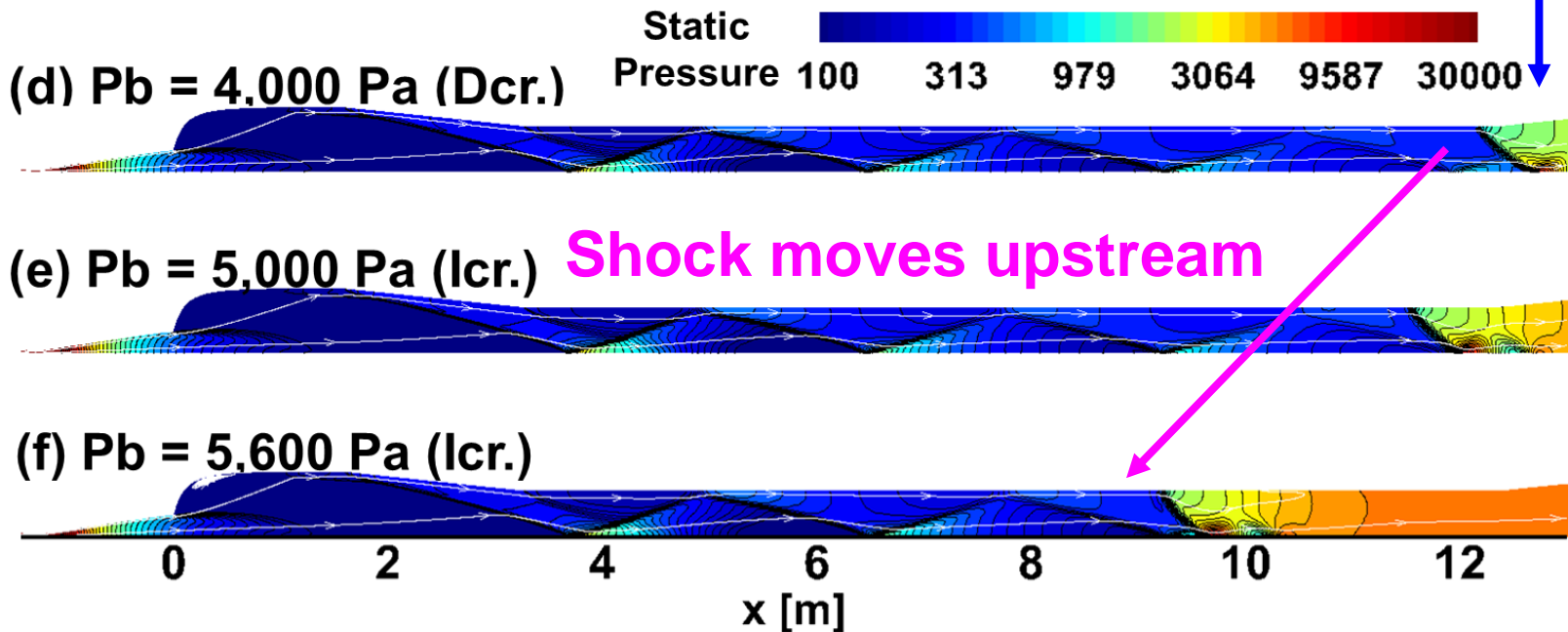
< Pressure distribution of nozzle and test section before starting >



# Varying Back-pressures

- Increasing back-pressure
  - After wind tunnel starting

“Swallowed”



< Pressure distribution with different back-pressure (Increasing) >



# Varying Back-pressures

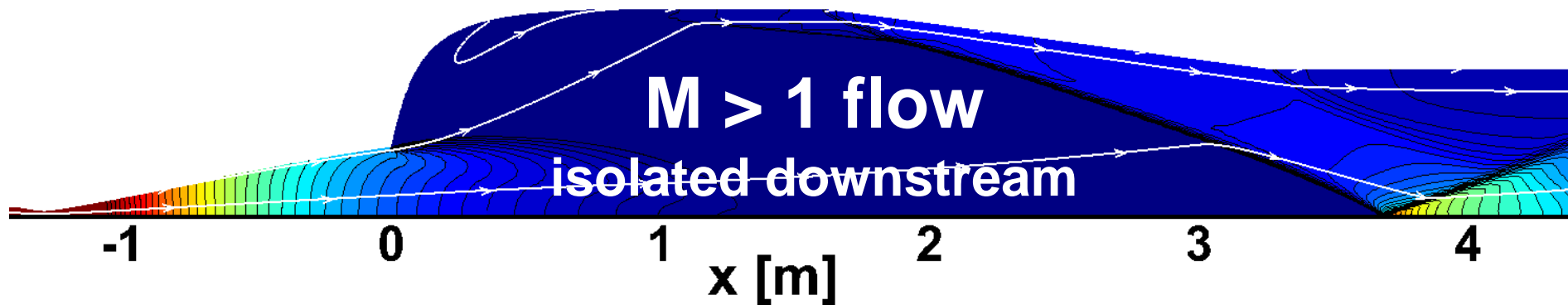
- Increasing back-pressure
  - Under-expanded flow at the nozzle exit
  - **TS isolated to downstream** condition

Static Pressure



100 313 979 3064 9587 30000

(e)  $P_b = 5,000 \text{ Pa}$  (lcr.)



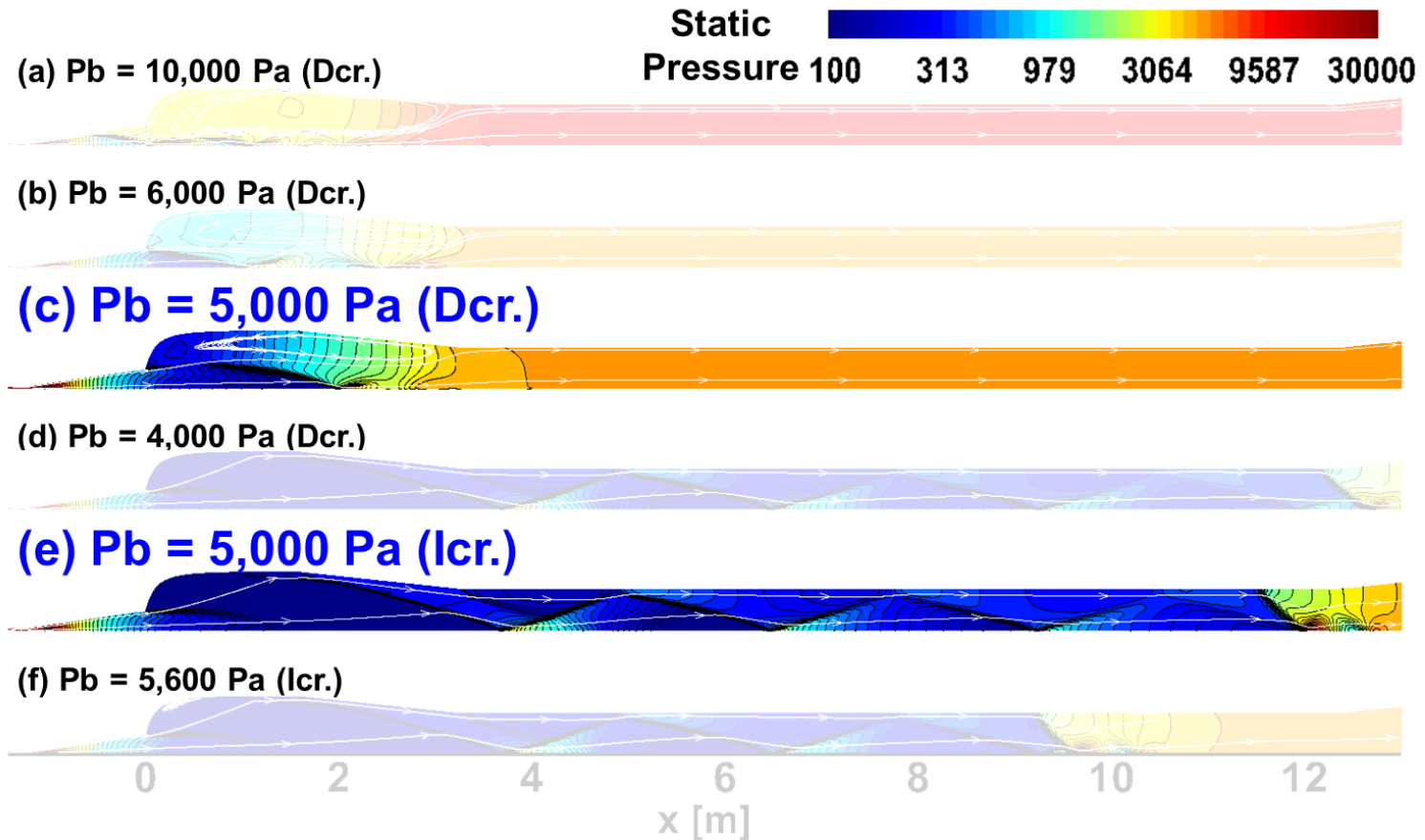
< Pressure distribution of nozzle and test section after starting >



# Starting Characteristics



# Starting Characteristics

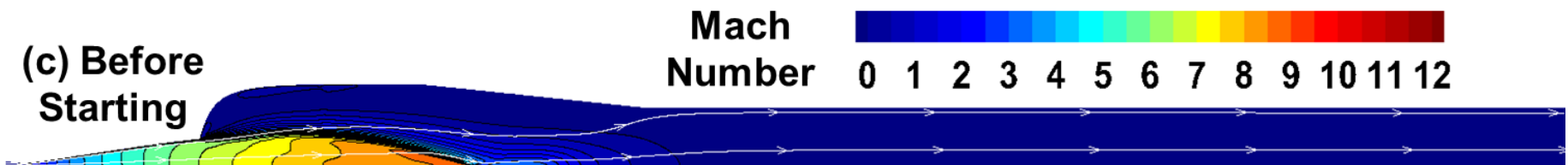
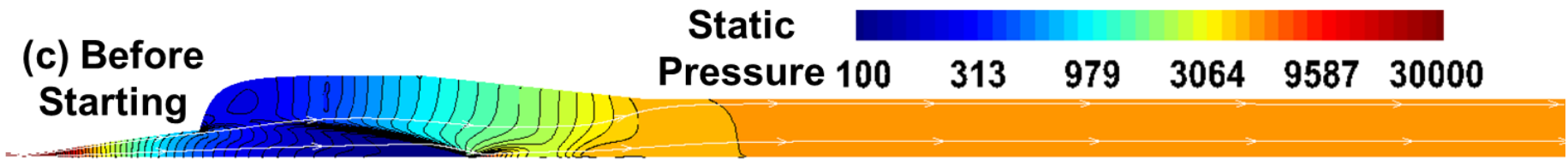


< Pressure distribution with different back-pressure >



# Starting Characteristics

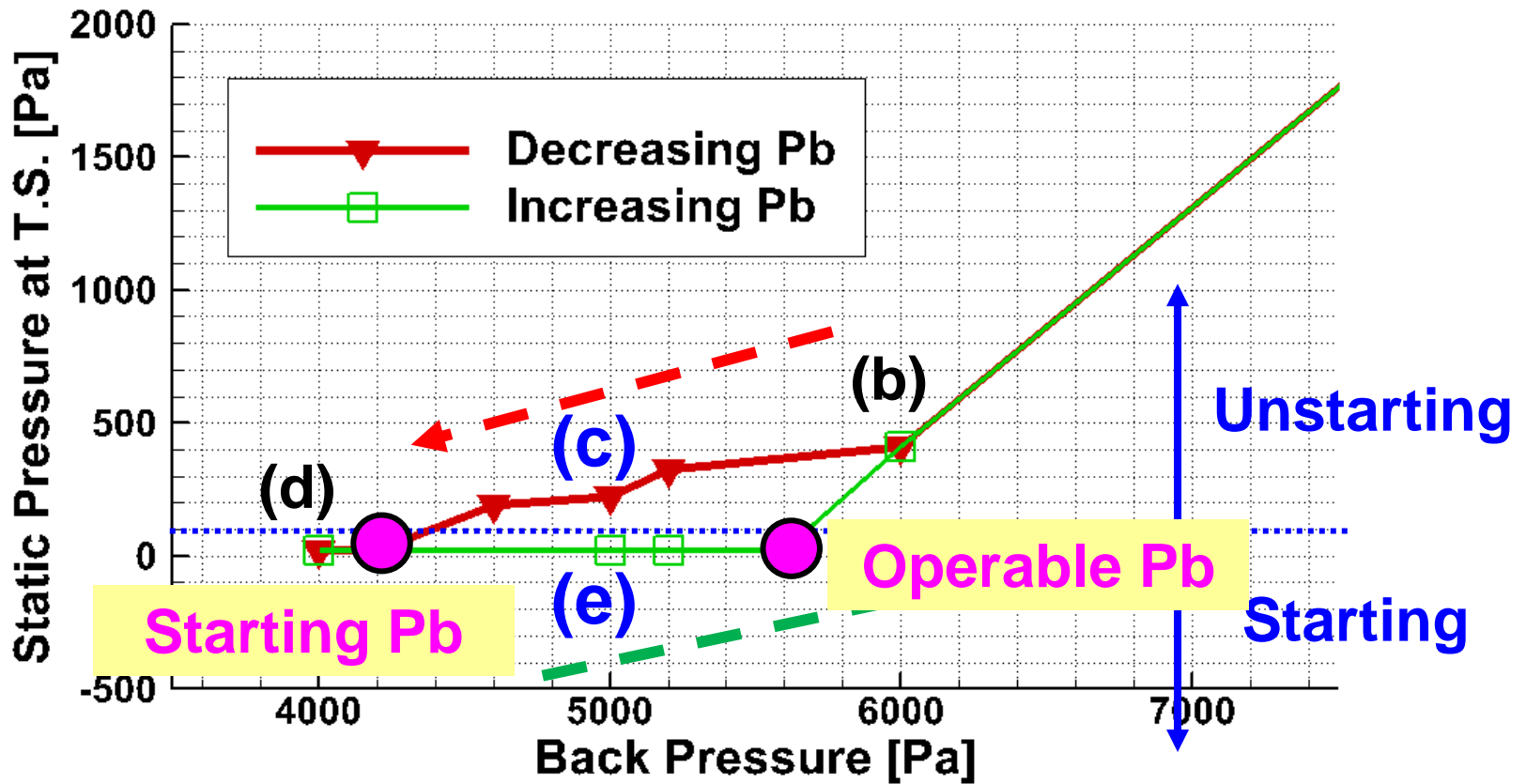
- **Hysteresis**
  - Dependence of the state on its history



< Different flow distribution at same back-pressure of 5,000 Pa >



# Starting / Operable back-pressure



< Pressure at TS ( $x = 0.5$  m) with different history of back-pressure >

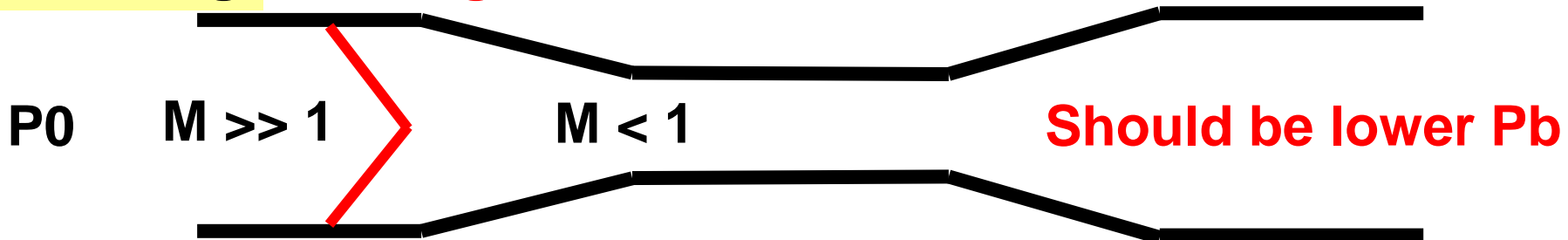


# Wind Tunnel Starting

- **Required pressure ratio ~ loss in PWT**
  - Loss in starting state < Loss in unstarting state

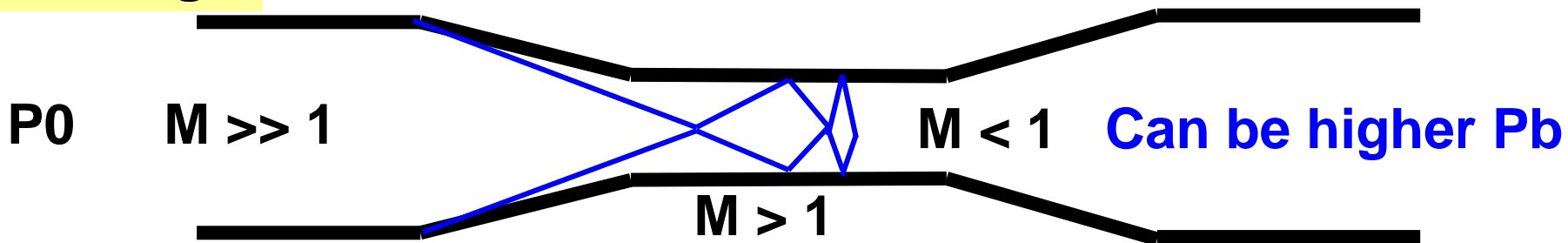
**Unstarting**

**Strong shock wave → severe loss**



**Starting**

**Series of weak shock waves → less loss**





# Conclusion



# Summary

- **Investigate the flow in PWT**
  - Identifying severe total pressure loss
- **Investigate starting characteristics**
  - Identifying
    - (1) Maximum operable back-pressure
    - (2) Starting back-pressure
    - (3) Hysteresis
  - Necessary to consider hysteresis



# Future Works

- **Unsteady calculation**
  - Considering starting scenario
  - Compare to step-by-step steady calculation
- **Study “Hot” flow condition**
  - Temperature  $> 4,000$  K
  - Nonequilibrium effect



**Thank you for your attention.**



# Reference



- **Type of Wind Tunnel - 5p**

[1] D. M. Smith, E.J. Felderman, F.L.Shope, (2002) 'Arc-Heated Facilities'

- **Characteristics of PWT - 6p**

[2] Savino, R., Monti, R. and Esposito, A. (1999) 'Behaviour of hypersonic wind tunnels diffusers at low Reynolds nwaabers', Aerospace Science and Technology, (1), pp. 11–19.

- **Characteristics of PWT - 7p**

[3] B. Monnerie, Study of a family of diffusers for a low-Reynolds-number hypersonic wind tunnel (Diffuser use in low density hypersonic wind tunnel and method of evaluating global performance for diffusers with conical inlet followed by cylindrical mixing section), LA RECH. AEROSP. (1967) 9–16.

[4] R.S Pugazenthi and Andy C. McIntosh (2011) 'Design and Performance Analysis of a Supersonic Diffuser for Plasma Wind Tunnel'. doi: doi.org/10.5281/zenodo.1330939.

[5] T.A. Shams, S.I.A. Shah, M.A. Ahmad, Capability Analysis of Global Hypersonic Wind Tunnel Facilities for Aero-thermodynamic Investigations, in: Proc. 2020 17th Int. Bhurban Conf. Appl. Sci. Technol. IBCAST 2020, 2020: pp. 481–501. <https://doi.org/10.1109/IBCAST47879.2020.9044523>.



- **Motivation - 8p**

[6] R. Monti, D. Paterna, R. Savino, A. Esposito, Low-Reynolds number supersonic diffuser for a plasma-heated wind tunnel, *Int. J. Therm. Sci.* 40 (2001) 804–815. DOI: 10.1016/S1290-0729(01)01267-4.

[7] A.J. Brune, S. Hosder, D. Campbell, S. Gulli, L. Maddalena, Numerical analysis of an actively cooled low-Reynolds-number hypersonic diffuser, *J. Thermophys. Heat Transf.* 33 (2019) 32–48. DOI: 10.2514/1.T5437.

- **Motivation - 9p**

[8] Agostinelli, P. W., Trifoni, E. and Savino, R. (2019) ‘Aerothermodynamic analyses and redesign of GHIBLI Plasma Wind Tunnel hypersonic diffuser’, *Aerospace Science and Technology*, 87, pp. 218–229. doi: 10.1016/j.ast.2019.02.023.

- **Modeling of Equilibrium - 17p**

[9] Anderson, J. D. (2006) *Hypersonic and High Temperature Gas Dynamics* (AIAA Education). American Institute of Aeronautics and Astronautics Inc, AIAA.



- **Modeling of Equilibrium - 19p**

[10] Srinivasan, S., Tannehill, J. C. and Weilmuenster, K. J. (1181) NASA Reference Simplified Curve Fits for the Thermodynamic Properties of Equilibrium Air.

[11] Gupta, R. N. et al. (1991) Calculations and Curve Fits of Thermodynamic and Transport Properties for Equilibrium Air to 30000K, NASA Reference Publication 1260.

- **Modeling of Turbulence - 20p**

[12] Jones, W. P. and Launder, B. E. (1972) 'The prediction of laminarization with a two-equation model of turbulence', International Journal of Heat and Mass Transfer, 15(2), pp. 301–314. doi: 10.1016/0017-9310(72)90076-2.

- **Computation - 21p**

[13] Kim, K. H., Kim, C. and Rho, O. H. (2001) 'Methods for the accurate computations of hypersonic flows. I. AUSMPW+ scheme', Journal of Computational Physics, 174(1), pp. 38–80. doi: 10.1006/jcph.2001.6873.

[14] Sweby, P. K. (1984) 'High Resolution Schemes Using Flux Limiters for Hyperbolic Conservation Laws', SIAM Journal on Numerical Analysis, 21(5), pp. 995–1011. doi: 10.1137/0721062.



- **Computation - 21p**

[15] Yoon, S. and Jameson, A. (1988) 'Lower-upper symmetric-gauss-seidel method for the euler and navier-stokes equations', AIAA Journal, 26(9), pp. 1025–1026. doi: 10.2514/3.10007.

- **Inflow / Boundary Conditions - 28p**

[16] Witte, D. W. et al. (2004) 998 Calibration of the Mach 4.7 and Mach 6 Arc-Heated Scramjet Test Facility Nozzles. Hampton, Virginia. Available at: <http://www.sti.nasa.gov>.